An antibody drug engineered for prevention of malaria in global populations

Katherine Williams (kwilliams@atreca.com)
Atreca, Inc.

Steve Guerrero
Atreca, Inc.

Yevel Flores-Garcia
Johns Hopkins Bloomberg School of Public Health

Kayla Andrews
Bill & Melinda Gates Medical Research Institute

Dongkyoon Kim
Initium Therapeutics

Kevin Williamson
Atreca, inc.

Christine Siska
Just – Evotec Biologics

Pauline Smidt
Just – Evotec Biologics

Sofia Jepson
Just – Evotec Biologics

Hong Liu
Bill & Melinda Gates Medical Research Institute

Kan Li
Duke Center for Human Systems Immunology

S Dennison
Duke University https://orcid.org/0000-0003-1198-9179

Shamika Mathis-Torres
Johns Hopkins Bloomberg School of Public Health

Xiaomu Chen
Agilent Technologies

Ulrike Wille-Reece
BioNTech US Inc.

Randall MacGill
PATH's Malaria Vaccine Initiative https://orcid.org/0000-0002-4566-1481

Michael Walker

Walker Bioscience
Erik Jongert
GlaxoSmithKline (Belgium)
C King
PATH Center for Vaccine Innovation and Access
Christian Ockenhouse
PATH Center for Vaccine Innovation and Access
Jacob Glanville
Centivax
James Moon
Center for Enabling Capabilities, Walter Reed Army Institute of Research
Jason Regules
Walter Reed Army Institute of Research
Yann Chong Tan
Nuevocor Pte. Ltd.
Guy Cavet
Paramune, Inc.
Shaun Lippow
Atreca, Inc.
William Robinson
Stanford University https://orcid.org/0000-0003-4385-704X
Sheetij Dutta
Walter Reed Army Institute of Research
Georgia Tomaras
Duke School of Medicine https://orcid.org/0000-0001-8076-1931
Fidel Zavala
Johns Hopkins University https://orcid.org/0000-0002-1414-6196
Randal Ketchem
Just – Evotec Biologics
Daniel Emerling (✉ **emerling@biosimplify.com**)
Atreca, Inc. https://orcid.org/0000-0002-8754-9201

Article

Keywords:

Posted Date: April 4th, 2023

DOI: https://doi.org/10.21203/rs.3.rs-2678519/v1

Abstract

Over 80% of malaria-attributable deaths are in children under five. However, the only malaria vaccine recommended by the World Health Organization (WHO) for paediatric use, Mosquirix™, has limited efficacy. Complementary strategies, like monoclonal antibodies (mAbs), will be required to eradicate malaria. To discover new anti-malaria mAbs, we evaluated >28,000 antibody sequences from circulating B cells obtained from 45 Mosquirix™ vaccinees and selected 369 for testing. Many antibodies bound the circumsporozoite protein (CSP), a main surface protein on malaria and the malaria antigen in Mosquirix™, and several were exceptionally protective in mouse models of malaria. Through this work, we identified surprising correlations that suggest certain CSP sequences in Mosquirix™ may induce immunodominant antibody responses that dilute protective immunity. Further, we selected the antibodies most protective in preclinical mouse models and engineered them for improved manufacturability and developability to meet WHO guidelines. An optimised clinical candidate, MAM01, suitable for paediatric populations living in low-to-middle-income countries, was selected for clinical development.

Introduction

Malaria is a mosquito-borne, parasitic disease endemic in regions impacting over 1.5 billion people in Asia, the Americas, the Middle East, and Africa. More than 247 million malaria cases and 619,000 malaria-related deaths were reported in 2021[1], with 76.8% of these deaths occurring in children under five. These data underscore the urgent need for prophylaxis, vaccines, treatments, and eventual eradication. Although vaccination has been a key tool in controlling and eradicating other infectious diseases, the development of a vaccine for malaria has been a half-century challenge[2]. The most advanced vaccine, and the only one recommended for use by the WHO, RTS,S/AS01 (Mosquirix™), targets the circumsporozoite protein (CSP) of *Plasmodium falciparum* (Pf), the malaria species primarily responsible for mortality in Africa[2]. Three immunisations with RTS,S/AS01 induce anti-PfCSP antibodies that act by binding to sporozoites, the infective form of the malaria parasite introduced by mosquito bite, and inhibiting their initial infection of liver cells[3,4]. However, the immune response induced by Mosquirix™ in children is limited to 45% vaccine efficacy against clinical malaria after the first dose, waning to 36% over 4 years of follow-up[5]. Thus, other immunisation approaches will be needed to achieve the WHO's goal of reducing the malaria case incidence and mortality rates by 90% by 2030[6].

Recent reports show that treatment with mAbs[7] can completely prevent malaria after controlled infection[8] and provide 88% efficacy for 6 months (prevention of infection) in an endemic region[9]. Thus, mAbs with durability lasting 4-6 months could provide an intervention with greater protective efficacy than seen with RTS,S, significantly aiding efforts to prevent seasonal transmission[10]. The mAbs tested in clinical trials, L9[11] and CIS43[8,9], were isolated from B cells of vaccinees immunised with whole sporozoites, and can prevent malaria infection by targeting specific epitopes on CSP. CSP comprises three main domains: i) an N-terminus; ii) a central repeat (CR) region composed of multiple (25–40) tetrapeptides of NANP ("major repeat") interspersed with an NPDP tetrapeptide and 2-4 NVDP ("minor repeat") tetrapeptides; and iii) a C-

terminal domain[12,13]. L9 and CIS43 preferentially bind epitopes containing, respectively, NPNV[14] in the minor repeat region and DPNA[15] in the "junctional region" (JR) that links the N-terminal and repeat domains. However, both mAbs can promiscuously bind NPNA epitopes in the CR region[14], which are conserved across all Pf strains[16,17] and are the only repeat tetrapeptides from CSP included in RTS,S. A third mAb, AB-000317[18], preferentially binds NPNA epitopes, and is reported to provide comparable maximum levels of protection as L9 and CIS43 in animal models[14,19].

Here we report on the isolation of AB-000317 and more than 50 other *in vivo* protective antibody lineages by deconstructing the anti-CSP humoral immune responses of RTS,S vaccinees. Despite the heterogeneous degree of protection that RTS,S provides, we identify antibody lineages that have protective activity and reveal that expression of these lineages by circulating antibody-secreting B cells (plasmablasts [PBs]) after the third dose of vaccine is not necessarily sufficient for protection. Given the published support for prophylaxis with mAbs as a strategy against malaria[8,9,11], and the productive advancement of mAbs as therapeutics and prophylactics against infectious diseases in general, we aimed to select and engineer a protective clone with biophysical properties amenable for cost-effective manufacturing and dosing in paediatric populations[20,21].

Results

PBs skewed to dominant, mutated immunoglobulin G lineages post-RTS,S vaccination

We sequenced the messenger RNA of immunoglobulin (Ig)G-expressing PBs isolated from peripheral blood mononuclear cells (PBMCs) of individuals (*n* = 45) vaccinated with RTS,S in a phase 2a clinical trial[22] using our Immune Repertoire Capture® sequencing platform. In this trial, participants either received three full doses of RTS,S/AS01$_E$ 1 month apart (012M; *n* = 15) or two full doses 1 month apart, followed by a smaller (one fifth, "fractional") dose 6 months later (Fx017M, *n* = 30). Vaccinees were challenged with malaria in a controlled human malaria infection (CHMI) model after the third dose. A subset received a fourth dose and were challenged a second time with malaria. PBs were isolated from PBMCs collected 7 days post-third (P3D; *n* = 22,319 PB) and post-fourth doses (P4D; *n* = 10,629 PB; Supplementary Table 1) prior to CHMI and were used to generate natively paired heavy and light chain IgG sequences. Almost all (99.2%) of the antibody sequences were divergent from inferred germline precursor sequences (Extended Data Fig. 1, *see Methods*). Consistent with previous malaria studies[15,23–26], specific germline heavy and light chain genes and pairings, including IGHV3-30/33, KV1-5, KV3-20, and LV1-40 were observed frequently in the dataset (Extended Data Fig. 2a–c). No significant associations were observed between protection status and multiple IgG sequence and repertoire features examined (Extended Data Fig. 2d–i).

P3D and P4D PBs were grouped into Ig lineages (*n* = 18,980), defined here as PB sequences that were likely derived from a common progenitor B-cell clone (*see Methods*). Lineage size ranged from 1–84 (P3D) or 1–93 (P4D) PBs. As PBs have a short half-life in blood[27] (reviewed in[28,29]) and were isolated

from a small volume of blood (~10 ml), detection of lineages with ≥2 PBs indicates recent expansion in lymphoid organs. One-fifth of lineages were cellularly expanded and contained at least two PBs with either the same or divergent B-cell nucleotide sequences (19.4%, *n* = 3,684 lineages, Fig. 1a). Consistent with antigen-driven selection pressure following vaccination, most of the cellularly expanded lineages also showed evidence of clonal expansion (Fig. 1b), a hallmark of affinity maturation. Furthermore, several lineages had clonal representatives that were observed after both the third and fourth immunisations, referred to here as "recalled" lineages (4.1%–26.6% of vaccinee P3D expanded lineages). In addition, when sequences were compared between the vaccinees, we observed that many of these expanded lineages also show evidence of sequence convergence between ≥2 vaccinees (7.3%–46.7% of vaccinee P3D expanded lineages, *see Methods*). Not surprisingly, lineages with only a single observed PB in P3D repertoires (*n* = 10,841) had significantly lower rates of convergence (2.0%–13.8%) and recall (1.2%–18.6%) than the expanded lineages ($P < 0.0001$ and $P < 0.001$, respectively, Wilcoxon matched-pairs, two-tailed test) and had higher levels of somatic hypermutation (SHM, Extended Data Fig. 3a). Thus, to increase the chances of identifying antibodies derived against RTS,S antigen, we mainly focused subsequent analyses on expanded lineages (Fig. 1b).

We hypothesised that lineages with the largest number of PBs per vaccinee, referred to here as "dominant lineages", were more likely to target the vaccine, as they had outcompeted other PB lineages for antigen binding and/or T-cell help in lymphoid organs. Thus, for each vaccinee, expanded P3D lineages (9–99 expanded lineages observed per vaccinee) were rank-ordered by size ("rank-size"). The sum of PBs in the lineages of the top four rank-sizes for each vaccinee constituted 17%–100% of the total number of PBs in each vaccinee's P3D repertoire of expanded lineages and 33% of the PBs among the P3D-expanded lineages from all vaccinees (Fig. 1c). Because this pattern of PB distribution was consistent across protection status and dose regimens (Extended Data Fig. 3b–c), we generated a mAb screening library for *in vitro* and *in vivo* characterisation that was biased toward the dominant P3D lineages of both protected and not protected vaccinees.

CSP-reactivity of expanded P3D PBs is associated with lower SHM and lack of protection

A clone from each of 369 unique P3D lineages was chosen, gene synthesised, and recombinantly expressed for testing (*see Methods*, Extended Data Fig. 4a). This library included almost all (96%) of the largest lineages (rank-size 1) across all vaccinees; approximately half (56%) of the second, third, and fourth rank-size lineages across all vaccinees; a small subset (6.9%) of expanded, sub-dominant lineages (rank-size ≥5), and a few single-PB lineages (0.18% of the 10,841 single-cell lineages). All mAbs were screened in a CSP enzyme-linked immunosorbent assay (ELISA) (Fig 1d, Extended Data Fig 4b), and approximately one-third were screened against the other RTS,S component, hepatitis B surface antigen (HBsAg, Extended Data Fig. 4c). Of the mAbs screened in both assays (*n* = 130), 52% were reactive to CSP (29/130) or HBsAg (39/130). In total, 38% (139/369) of all mAbs bound to CSP, and binding for an additional 29 mAbs was indeterminate. Of the CSP-reactive mAbs, 73% (102/139) bound peptides from the NANP CR region and 14% (20/139) bound peptides from the C-terminal region (Supplementary Table 2).

Given that expanded lineages were more likely to show evidence of convergence and recall as compared to single PBs, we tested whether those same features were associated with CSP-reactivity. Indeed, mAbs from lineages that show sequence convergence across ≥2 vaccinees were more likely to bind to CSP (54%, 55/102) than clones from lineages that lacked evidence of convergence (31%, 84/267, $P = 0.0001$, Fisher's exact, two-sided). Recalled lineages were also more likely to be CSP-reactive (49%, 43/87) as compared to lineages only observed P3D (19%, 16/83 $P < 0.0001$, Fisher's exact).

Similar to other reports describing immunisation with whole sporozoites[25–28], we found SHM levels of CSP-reactive mAbs were significantly lower than SHM levels of CSP non-reactive mAbs ($P < 0.0001$, Fig. 1d), and SHM levels of NANP-specific mAbs were lower than SHM levels of C-terminal binding mAbs ($P < 0.006$, Fig.1d). Consistent with our previous observations about these sequence repertoires[16], SHM levels of NANP-binding mAbs were not correlated with vaccinee protection status P3D ($P > 0.6$, Extended Data Fig. 5b). Further, the percentage of mAbs that were CSP-specific and NANP-specific was surprisingly lower among P3D-protected vaccinees than P3D-non-protected vaccinees ($P < 0.0007$ for CSP, $P < 0.006$ for NANP, Fisher's exact, Fig. 1e–f). This inverse correlation between mAb binding and P3D protection status is also observed when the analysis is restricted to just the mAbs from the most dominant lineages (rank-size 1–4, $P < 0.0004$, Fig. 1g), as well as when all mAbs, including the 20 from lineages that have only 1 PB, are combined in the analysis ($P < 0.0005$ Fisher's exact and $P = 0.001$ by bootstrap analysis, Fig. 1h). These data suggest that the quality of the CSP-specific antibody repertoire may be more important in driving protection than the overall quantity of circulating, CSP- or repeat-specific PBs.

Sporozoite inhibitory antibodies in P3D PBs are not sufficient for P3D protection

Given this surprising inverse association and the well-reported protective activity of CSP-binding mAbs in both humans[8,11] and mice[15,18,23,24,30,31], we selected mAbs to advance as potential anti-malaria prophylactics without assuming any correlate of protection. Seventy-seven mAbs (77 unique lineages) were selected that included NANP- and C-terminal-reactive mAbs from protected ($n = 26$) and not protected ($n = 8$) vaccinees, and from dominant and sub-dominant lineages of either high or low SHM levels (respectively, ≥20 or <20 nucleotide mutations from germline per antibody, *see Methods*). As *in vitro* functional assays have demonstrated limited predictive power for *in vivo*, anti-malaria activity[14,31], we screened for activity using a mouse sporozoite-infection model[19,32]. Over half of these mAbs (44/77) provided ≥95% inhibition of sporozoite liver burden, and some offered near-complete protection (≥99.9% inhibition). All 44 mAbs bound the NANP-repeat region of CSP and most were derived from the IGHV3-33 germline, while some came from other IGHV3 genes, and one from IGHV1. Thirteen other NANP binding, IGHV3-30/33 mAbs demonstrated limited inhibition of parasite liver burden (80%–95%), and 12 mAbs, including three C-terminal peptide binders, showed minimal, but detectable inhibition (20%–80%, Fig. 2a, Supplementary Table 2).

Roughly a third of the tested mAbs (30%, 23/77) were from not protected vaccinees, including half (7/14) that showed near-complete protection in mice (≥99.9% inhibition, Fig. 2a). These data suggest expression of these inhibitory antibodies by circulating, expanded P3D PB lineages is insufficient to drive

protection. For example, the highly effective antibody AB-000317[18] is observed in both a protected vaccinee and a not protected vaccinee (Fig 1h, red circles). However, PB expansion levels for this antibody lineage differed between the two vaccinees. In the protected vaccinee, the antibody was a member of the largest PB lineage, while in the not protected vaccinee, the antibody was expressed in the seventh rank-size lineage (respectively, 15.8% versus 1.7% of PB in expanded P3D lineages, and 10% versus 0.9% of all circulating P3D PBs). These data are consistent with the hypothesis that, in addition to the functional activity of an antibody, the number of PBs expressing the antibody may affect protection status by ultimately influencing titre in blood and/or representation in immune memory[27,28,33–35].

Inhibitory antibodies from vaccinees bind CSP peptides not present in RTS,S

To explore the developability of these inhibitory mAbs as potential drugs, 35 NANP-repeat-binding lineages were selected for further pharmacology studies from the 52 that demonstrated ≥90% inhibition in the sporozoite-challenge screen. To avoid sequence features that can potentially act as liabilities during the development of mAb drugs, and to survey clones from lineages that have extensive clonal diversity, more than one unique antibody clone was chosen from some (n = 23) lineages. Overall, up to 141 mAbs, from 21 protected vaccinees of both RTS,S dose regimens, representing a range of high and low SHM levels, were tested in binding assays.

Antibodies displayed a broad range of affinities against CSP (K_D by surface plasmon resonance [SPR] of 11 pM–9.8 nM, Fig. 2b, Supplementary Table 3). Despite the inverse correlation observed between vaccinee protection status and the percentage of CSP-reactive mAbs observed in the original screening library (Fig. 1e–h), these down-selected, inhibitory mAbs had a significant association between CSP-binding affinity (K_D) and SHM levels (P < 0.005, r = −0.26 and P < 0.0001, r = −0.39 for heavy and light chain, respectively, Spearman test), indicating that affinity maturation to CSP occurred following vaccination. These correlations are likely driven by two relationships: binding association rates (k_{on}) to CSP and heavy and light chain SHM levels (Extended Data Fig. 6a–b; Extended Data Table 1) and binding dissociation rates (k_{off}) from CSP and SHM levels in the light chain (P < 0.0005, r = −0.29, Spearman; Extended Data Table 1).

Antibodies were also evaluated for binding to short (12–15 residues) and long (20–24 residues) peptides derived from the varied tetrapeptide-based epitopes (NPNA, NPNV, DPNA)[14,15,18,24,26,31,36,37] of the CSP CR and JR (Fig. 2b). Short peptides that were tested included an NPNA-containing major repeat-peptide homologous to epitopes in RTS,S, and two peptides heterologous to RTS,S, a DPNA/NPNV-containing minor repeat-peptide and a DPNA-containing JR peptide. Long peptides tested included an NPNA-containing peptide homologous to RTS,S, and a DPNA/NPNV-containing peptide heterologous to RTS,S. These peptide binding data show correlations between SHM and both k_{on} and k_{off}, with relatively greater coefficients, in some cases, than those seen with CSP (Extended Data Table 1). Specifically, higher levels of SHM are correlated with slower k_{off} to short peptides from both repeat and JR (Fig. 2c–e), while correlations with longer peptides have generally smaller coefficients (Fig. 2f–g, Extended Data Table 1).

Indeed, the strongest correlation was observed between SHM and binding rates to the short, homologous peptide even though the long version of the homologous peptide contains more repeats of the same epitope (Extended Data Table 1).

Furthermore, correlations between SHM levels and binding rates to the JR peptide, which is heterologous to epitopes in RTS,S, were stronger than for the long homologous peptide (Extended Data Table 1). These data indicate that B cell receptor maturation of these highly functional mAbs may have been preferentially driven by interactions with short versus long NANP epitopes that benefited maturation to heterologous peptide sequences. In addition, these observations are consistent with reports that some anti-CSP protective mAbs display promiscuous binding across distinct CSP epitopes[14,18,24,26,31,36,38], although other reports indicate that such promiscuity may not be required[31].

Anti-sporozoite activity correlates with CSP-peptide binding and SHM levels

Seventy mAbs, representing 33 of the 35 protective lineages evaluated in binding studies, were directly compared in an intravenous sporozoite-challenge mouse model to the highly efficacious mAb AB-000317[18,19,26,31,37,39–41] in order to prioritise inhibitory, mAbs for development as anti-malaria drugs. Antibodies inhibited 44.1%–97.5% of sporozoite liver burden (47.4%–103.8% of AB-000317 inhibition, Supplementary Table 3). Overall, about half of the mAbs demonstrated inhibition comparable to AB-000317 (n = 32), while the other half demonstrated significantly weaker inhibition (n = 36), and one, AB-000224, showed activity that was superior to AB-000317 (Fig. 3a–b, Supplementary Table 3). Serum concentrations for most mAbs were at least 1000-fold higher than the CSP K_D of the respective mAbs (Supplementary Table 3, Fig. 3c), indicating that antibodies demonstrating weak inhibition were not likely due to low levels of circulating antibody. Lineages with at least one mAb that demonstrated activity consistent with AB-000317 were considered for further advancement.

To determine if RTS,S-driven affinity maturation contributed to mAb inhibition, we assessed whether percent inhibition compared to AB-000317 correlated with peptide binding kinetics or SHM levels. Indeed, relative activity was associated with slower k_{off} from CSP (Fig. 3d), with slower k_{off} from the short homologous peptide, NPNA3 (Fig. 3e), and with slower k_{off} from the JR and the other short, heterologous peptide (Fig. 3f–g, Extended Data Table 1). Strikingly, no significant correlations were observed between inhibitory activity and binding kinetics with the long homologous peptide, NANP6 ($P > 0.3$ [k_{off}]; $P > 0.7$ [k_{on}], Spearman and Pearson, Extended Data Table 1), despite this peptide being the most representative of both RTS,S and CSP. Taken together, the data evaluating these inhibitory antibodies suggest that while binding to NPNA epitopes may be required[31], mutations which favour binding to heterologous peptides may be preferred over mutations that simply improve binding to the longer, homologous NPNA epitopes[36,42].

Indeed, affinity maturation via SHM likely underlies the correlations between *in vivo* function and binding kinetics, as inhibitory activity significantly correlates with heavy and light chain nucleotide and amino acid changes from germline (Fig. 3h–i, Extended Data Table 1). Consistent with this observation, low

SHM mAbs were more likely to demonstrate significantly weaker inhibition compared to AB-000317 than mAbs with higher mutational burden (86% [12/14], versus 44% [24/55], $P = 0.007$; Fisher's exact, two-sided). Taken together, these correlations between higher SHM levels and binding kinetics to homologous (Fig. 2c, f) and heterologous epitopes (Fig. 2d–e, g), and between higher SHM levels and inhibitory activity (Fig. 3h–i), suggest that affinity maturation to epitopes of RTS,S includes bystander maturation to heterologous epitopes that may be functionally important.

Despite the correlations between SHM levels, inhibitory activity, and k_{off} from CSP and short peptides, some mAbs with high SHM levels are exceptions. In some cases, high SHM mAbs have relatively fast k_{off}, and slow k_{on}, and are comparatively poor inhibitors like many of the low SHM mAbs (Fig. 3j). These antibodies may have resulted from inefficient affinity maturation and/or aberrant selection mechanisms limiting survival in and recall from memory[36,43–46] (Fig. 1e–h). In other cases, some high SHM mAbs have relatively fast k_{off} and slow k_{on} to short peptides but are still relatively good inhibitors despite their unfavourable binding kinetics (Fig. 3j). In these latter cases, affinity maturation toward antibody homotypic Fab–Fab interactions, not CSP epitopes, may contribute to the relatively strong activity. Inter-antibody binding events can contribute to anti-CSP-binding potency and increased functional activity[25,47], and have been reported for some mAbs described here[41,47] (*Martin et al., 2022, https://www.biorxiv.org/content/10.1101/2022.09.20.508747v1, in review with Nature Communications*). Such homotypic interactions may not be reflected in binding kinetics to short NPNA3 peptides, which due to their short length, cannot sterically accommodate multiple simultaneous binding events [25,47] (*Martin et al., 2022, https://www.biorxiv.org/content/10.1101/2022.09.20.508747v1, in review with Nature Communications*). Indeed, four mAbs that have relatively fast k_{off} to short peptides, but are comparable to AB-000317 in activity, are from a lineage containing a mAb that binds via Fab–Fab homotypic interactions (AB-000399[41], Fig. 3j, red circles) (*Martin et al., 2022, https://www.biorxiv.org/content/10.1101/2022.09.20.508747v1, in review with Nature Communications*). Overall, the data are consistent with mAb affinity maturation via multiple different modes of binding[18,39,41,47], and reveal several mAbs (>30) with activity comparable to that of AB-000317 and the potential to be developed into clinical leads.

Lead antibodies prioritised for development

To identify the most optimal lineage(s) for clinical candidate development, we compared mAbs for pharmacological and developability characteristics. Using the sporozoite liver burden data, we further down-selected 26 mAbs representing 15 lineages for evaluation in the parasitaemia challenge model as an alternate endpoint for assessing *in vivo* function[19,32]. This set included AB-000317, AB-000224, 23 other mAbs with liver burden inhibitory activity similar to AB-000317, and one mAb with weaker activity than AB-000317. All except two mAbs were significantly more likely to prevent parasitaemia than the negative control, yet no mAbs were significantly better than AB-000317 (Supplementary Table 3). Serum concentrations for almost all mAbs (25/26) at the time of infection were at least 1000-fold higher than the respective mAb's $K_{D\text{CSP-SPR}}$ (Supplementary Table 3), indicating that mAbs more efficacious than AB-

000317 were likely not missed due to low levels of circulating antibody. Overall, the data suggest that AB-000317 has *in vivo* activity at or near maximal efficacy among this set of lead antibodies. Seven mAbs displayed a trend towards superior protection versus AB-000317 (non-parametric log-rank hazard ratios <1 versus AB-000317, Fig. 3k, Supplementary Table 3). Three of these mAbs belonged to the AB-000224 lineage, the only mAb that demonstrated significantly better activity than AB-000317 in the liver burden model (Fig. 3a–b). Given these functional assessments, AB-000224 was considered the prime lead molecule. Only one other mAb from a separate lineage, AB-007088, demonstrated a similar trend to superiority over AB-000317 in a repeated parasitaemia challenge experiment (Fig. 3l, Supplementary Table 3).

A subset of antibodies (19 mAbs from 14 lineages) evaluated in the parasitaemia model was also compared for drug properties important in developing medicines[48], including biophysical characterisation assays relevant to drug stability (i.e., protein conformational and solution colloidal stability, *see Methods*). Although none of the data indicate any of the leads should be eliminated as potential drugs due to definitive development risks, the prime lead, AB-000224, and its siblings, generally performed less favourably than many other mAbs in several assays (Fig. 4a–b). Thus, we selected AB-007088 as a backup molecule given its more favourable biophysical characteristics (Fig. 4b) and efficacy (Fig. 3k–l).

Clinical candidate engineered for optimised developability

While functional potency is essential for any effective drug, biophysical properties like manufacturability, stability and formulation are equally critical for successful drug development. Because our lead antibodies demonstrated protective *in vivo* activity comparable to AB-000317, we prioritized improving biophysical stability and cell line manufacturing properties by mutating specific residues in the antibody framework regions per Just – Evotec Biologics' Abacus™ design platform without impacting mAb activity (Fig. 4c–d, *see Methods*). For AB-000224 and AB-007088, a total of 17 and 5 clonal variants, respectively, were engineered and tested in the same biophysical and pharmacologic assays used previously.

Importantly, engineered mutations improved both conformational and colloidal stability of many variants, including enhanced thermal stability, solubility, and aggregation profiles during storage (Fig. 4e–h). Most of the variants retained parental mAb binding profiles against a subset of tested peptides ($NPNA_3$ and $NVDP_2NANP_3$; Extended Data Table 2). Like the parental mAbs, activity was not significantly different than AB-000317 for the subset that was tested in the parasitaemia challenge model; however, unlike the previous screening result that showed AB-000224 to be more efficacious than AB-000317 in the liver burden model (Fig 3b), average percent inhibition for almost all variants of AB-000224 was comparable to AB-000317 across repeated experiments (Extended Data Fig. 7 and Extended Data Table 3). As sera concentrations of the variants at the time of challenge were consistently lower than those of AB-000317 (Extended Data Table 3), mutations engineered in the variants were unlikely to contribute to a reduction in functional activity compared to the parental mAbs. Variants generated as human IgG1 with an Fc mutation to extend half-life (Xtend[49]) were used to make a panel of stable transfectant cells. Expression and metabolic data were collected (Fig. 4i–j and Extended Data Fig. 8) to identify the best pools for the

generation of a production cell line (*see Methods*). Optimisation of stability violations in AB-000224 greatly improved production titres (Fig. 4i), which importantly, can reduce cost per dose. Three cell lines from the panel of 22 variants were selected for clone generation. The top clonal cell line from one of the engineered mAbs, MAM01, advanced into production following good manufacturing practices (GMP) to support studies for a clinical development of an anti-malaria drug suitable for use in paediatric populations living in low-middle income countries (LMICs).

Discussion

Using single-cell sequencing of B cells from RTS,S vaccinees, we generated a library of natural, CSP-specific mAbs that could be assessed and down-selected to those most amenable for engineering and development as anti-malaria medicines. In doing so, we also uncovered important characteristics of the humoral response to RTS,S that may underlie this vaccine's efficacy and durability.

First, we unexpectedly discovered an inverse relationship between the percentage of CSP-specific IgG-expressing PBs and protection P3D (Fig. 1e–h). These data suggest that, despite the well-reported association between anti-CSP antibodies and protection, more cells expressing anti-CSP, NANP repeat-binding antibodies may not drive greater protection[50–54]. Since antibodies targeting the repeat regions display differing capabilities to inhibit sporozoites effectively, the difference between protective and not protective responses could be the result of the relative proportion of ineffective versus inhibitory NANP-binding antibodies. This point is exemplified by the highly efficacious mAb, AB-000317, which is expressed in the most dominant P3D lineage of a protected vaccinee and a much less frequent lineage of a not protected vaccinee (Fig. 1h). This inverse correlation between protection and prevalence of repeat-binding lineages (Fig. 1f) could result from competition between highly functional and weakly functional antibodies at the sporozoite surface ("epitope masking")[40,44,45], and/or within lymphoid organs[43], whereby dominant lineages of weakly functional antibodies out-compete sub-dominant, highly effective antibodies for binding to the repeat regions. In fact, our data indicating the P3D PB repeat-binding mAbs have lower levels of SHM than other mAbs (Fig. 1d) support the hypothesis that immature clones are preferentially activated and expanded over more protective memory clones[43,45,46] in lymphoid tissues. Furthermore, this hypothesis could underlie observations of RTS,S vaccination reported elsewhere that functional antibodies in sera were higher post-second dose (P2D) versus P3D[50], that anti-CSP P2D, but not P3D, PB and memory B cells associate with P3D protection status[55], and that some vaccinees lost prior protective immune signatures after receiving the third dose of RTS,S[55]. Overall, we propose that the simple presence of potent, inhibitory antibodies by P3D PBs is insufficient for protection. Rather relative levels of such antibodies versus other repeat-binding antibodies may be important in providing consistent protection.

Second, we found mAb protective activity *in vivo* does not correlate with binding kinetics to the long NANP6 peptide (Extended Data Table 1) but does significantly correlate with k_{off} to CSP and with binding kinetics to both the short NANP-containing peptide (NPNA3) and tetrapeptides of minor repeat and JR

(Fig. 3d–g, Extended Data Table 1). These data suggest that protective antibodies induced following RTS,S vaccination affinity mature to short NANP repeats but also gain or retain promiscuous binding activity to the minor repeat and junctional epitopes which are not present in RTS,S. Consistent with this interpretation, aggregate levels of SHM in both heavy and light chains of protective mAbs are correlated with binding kinetics to NANP-, NVDP-, and NPDP-containing short peptides (Fig. 2c–e, Extended Data Table 1) as well as with inhibitory activity in the sporozoite-challenge model (Fig 3h–i, Extended Data Table 1). Thus, both SHM levels and *in vivo* activity correlate with binding to short peptides that are included and not included in RTS,S, yet only SHM levels but not *in vivo* activity are correlated with binding to long NANP-repeat peptides. These observations are consistent with suggestions that next-generation anti-CSP vaccines should contain fewer NANP repeats[36,56] and/or include sequences from minor repeat and junctional regions[14,26,31,42,57–60], neither of which are included in RTS,S.

Lastly, multiple observations, including i) the correlation between *in vivo* activity and binding kinetics with NVDP- and NPDP-containing peptides absent in RTS,S (Fig 3f–g, Extended Data Table 1); ii) the correlation between *in vivo* activity and binding kinetics to the short NPNA3 but not the longer NANP6 peptide (Fig. 3e, Extended Data Table 1); and iii) the inverse relationship between NANP6-reactivity of expanded antibody lineages and protection against CHMI (Fig. 1f), are consistent with a hypothesis where multiple NANP repeats act as an immune "decoy"[36,61,62]. Under this hypothesis, antibody lineages that solely bind to NANP repeat-region epitopes, but provide limited protection, are preferentially expanded, diluting the protective capacity of the broader anti-CSP repertoire[36,43,45]. Whereas promiscuous mAbs which also bind to multiple NANP repeats and similarly exist at a high density on CSP, could further enhance mAb on-rates to heterologous epitopes. Thus, avidity afforded by promiscuous binding could drive more protective responses *in vivo*.

By sequencing PBs, which represent the breadth of Ig sequence diversity that originates from lymphoid reactions following RTS,S vaccination, we were able to deconstruct the humoral response of both protected and not protected vaccinees. We identified lineages with highly protective clones in mouse models, screened sequence-diverse clones within those lineages for development-related properties, and further engineered a clone to optimise its developability characteristics. These properties will increase the likelihood that dosing regimens can be successfully developed for paediatric populations, who require small volume, concentrated doses. Given that the *in* vivo efficacy displayed by MAM01 is comparable to AB-000317, which in turn has activity comparable to CIS43[14], we believe that MAM01 will be useful for individuals living in malaria-naïve and malaria-endemic regions. Like CIS43[9], MAM01 would enable 4-6 months of malaria prevention with ≥80% efficacy but would also meet the WHO's preferred product profile[21] that includes cost-effective dosing for delivery in LMICs. By focusing on properties critical for manufacturing and distribution to global paediatric populations[20,21], in addition to the requirement for functional potency, the work reported here may significantly contribute to prophylactic strategies that aid efforts to eradicate malaria.

Data Availability

Paired IgG sequence repertoire datasets The entire set of natively paired IgG sequences (*n* = 28,672) from PBs (*n* = 32,948) of RTS,S vaccines (*n* = 45) will be available at the site [*website provided upon publication*] as of [*date provided upon publication*]. Data annotations and formats are based on AIRR Community Standards (https://docs.airr-community.org/en/stable/index.html).

Other datasets generated during and/or analysed during the current study are available from the corresponding authors on reasonable request.

Data from the clinical trial of RTS,S are reported elsewhere [Regules, J. A. *et al.* Fractional third and fourth dose of RTS,S/AS01 malaria candidate vaccine: A phase 2a controlled human malaria parasite infection and immunogenicity study. *J. Infect. Dis.* **214**, 762–771 (2016)].

Code availability Custom code used in R for bootstrap analyses will be provided upon request.

All materials used in the study are commercially available except PBMC samples obtained from the clinical trial cited above, which were completely consumed in the course of the study, and the antibodies discovered in the study that were expressed as recombinant proteins and can be obtained via gene synthesis and recombinant expression using IgG sequence data and methods (see *Paired IgG sequence repertoire datasets* above and *Methods section, "Recombinant antibody production"*).

Declarations

Acknowledgements We thank Jacqueline Kirchner for scientific, business and leadership contributions and for manuscript review and editing; Lynda M. Stuart for scientific, business and leadership contributions; Laura Shackelton for scientific, business and project management contributions; Deborah Hopkins for project management contributions; R. Scott Miller for manuscript review and editing; Tito A. Serafini for corporate support and business and scientific contributions; Stephen E. Gould for manuscript review and editing and scientific contributions; Sarah Mudrak for project management support, manuscript review and editing; Ashley Birkett and Lode Schuerman for manuscript review and editing; F.Z., Y.F-G. and S.M-T. thank the Insectary Core of the Malaria Research Institute and the Bloomberg Philanthropies for continued support. This work was supported by the Bill and Melinda Gates Foundation (BMGF) at Atreca, Inc. and at Just – Evotec Biologics, Inc. [INV-008062] and with grants to F.Z. (INV-001763) and to G.D.T (OPP1151372 and INV008612) and by PATH-MVI with grant to F.Z. The contents of this publication are solely the responsibility of the authors and do not represent the official views of the Bill and Melinda Gates Foundation. We also acknowledge editorial assistance from Megan Hyde, PharmD and John McGuire, PhD, at BOLDSCIENCE Inc.

Author contributions Conceptualisation, K.L.W. and D.E.E. Methodology, K.L.W., S.G., Y.F-G., K.A., D.K., K.S.W., C.S., P.S., S.J., K.L., S.M.D., S.M-T., X.C., U.W-R., M.W., E.J., C.R.K., C.O., J.G., J.E.M., J.A.R., Y-C.T., G.C., S.M.L., W.H.R., G.D.T., F.Z., R.R.K., D.E.E.; Software, S.G.; Validation, K.L.W., S.G., Y.F-G., K.A., D.K.,

K.S.W., C.S., P.S., S.J., H.L., K.L R.S.M., S.D., R.R.K., D.E.E.; Formal Analysis, K.L.W., S.G., Y.F-G., D.K., K.S.W., C.S., P.S., S.J., K.L., S.M.D., U.W-R., M.W., R.S.M., C.O., J.G., S.D., Y.C.T., S.M.L., W.H.R., G.D.T., F.Z., R.R.K., D.E.E.; Resources, K.L.W., S.G., Y.F-G., K.A., C.S., P.S., S.D., G.D.T., F.Z., R.R.K., D.E.E.; Data Curation, K.L.W., S.G., Y.F-G., K.A., D.K., K.S.W., C.S., P.S., S.J., H.L., K.L., R.S.M., S.D., R.R.K., D.E.E.; Writing – Original Draft, K.L.W. and D.E.E.; Writing – Review & Editing, K.L.W., D.K., K.S.W., C.S., P.S., S.J., K.L., S.M.D., M.W., E.J., R.S.M., C.R.K, C.O., J.G., G.C., S.M.L., S.D., G.D.T., F.Z., R.R.K., D.E.E.; Project Administration, K.L.W. and D.E.E.

Competing interests W.H.R. owns equity in, serves as a consultant to, and is a member of the Board of Directors of Atreca, Inc. K.L.W., S.G., K.S.W., and S.M.L. own equity in and are employed by Atreca, Inc. D.E.E. and M.W. own equity in and serve as consultants to Atreca, Inc. G.C. owns equity in Atreca, Inc. C.S., P.S., S.J., and R.R.K. are employed by Just – Evotec Biologics. E.J. owns equity in and is employed by GSK. U.W-R. is employed by BioNTech. J.G. owns equity in, is employed by, and is a member of the Board of Directors of Centivax, Inc. Y.C.T. owns equity in Atreca and is employed by Nuevocor Pte. Ltd. K.L.W., S.M.L., R.R.K., and D.E.E. are coinventors on patent applications filed by Atreca, Inc. that include antibodies to CSP. The remaining authors declare no competing interests.

References

1. World Health Organization. *World malaria report 2022*. (World Health Organization, 2022).
2. Sinnis, P. & Fidock, D. A. The RTS,S vaccine—a chance to regain the upper hand against malaria? *Cell* **185**, 750–754 (2022).
3. March, S. *et al.* A microscale human liver platform that supports the hepatic stages of Plasmodium falciparum and vivax. *Cell Host Microbe* **14**, 104–115 (2013).
4. Campo, J. J. *et al.* RTS,S vaccination is associated with serologic evidence of decreased exposure to Plasmodium falciparum liver- and blood-stage parasites. *Mol. Cell Proteomics* **14**, 519–531 (2015).
5. RTS,S Clinical Trials Partnership. Efficacy and safety of RTS,S/AS01 malaria vaccine with or without a booster dose in infants and children in Africa: final results of a phase 3, individually randomised, controlled trial. *Lancet* **386**, 31–45 (2015).
6. World Health Organization. *Global technical strategy for malaria 2016-2030, 2021 update*. (World Health Organization, 2021).
7. Daily, J. P. Monoclonal antibodies — A different approach to combat malaria. *N. Engl. J. Med.* **387**, 460–461 (2022).
8. Gaudinski, M. R. *et al.* A monoclonal antibody for malaria prevention. *N. Engl. J. Med*. **385**, 803–814 (2021).
9. Kayentao, K. *et al.* Safety and efficacy of a monoclonal antibody against malaria in Mali. *N. Engl. J. Med.* **387**, 1833–1842 (2022).
10. Birkett, A., Miller, R. S. & Soisson, L. A. The Importance of Exercising Caution When Comparing Results from Malaria Vaccines Administered on the EPI Schedule and on a Seasonal Schedule. *Am.*

J. Trop. Med. Hyg. **107**, 1356 (2022).

11. Wu, R. L. *et al.* Low-dose subcutaneous or intravenous monoclonal antibody to prevent malaria. *N. Engl. J. Med.* **387**, 397–407 (2022).
12. Dame, J. B. *et al.* Structure of the gene encoding the immunodominant surface antigen on the sporozoite of the human malaria parasite *Plasmodium falciparum*. *Science* **225**, 593–599 (1984).
13. Zavala, F., Cochrane, A. H., Nardin, E. H., Nussenzweig, R. S. & Nussenzweig, V. Circumsporozoite proteins of malaria parasites contain a single immunodominant region with two or more identical epitopes. *J. Exp. Med.* **157**, 1947–1957 (1983).
14. Wang, L. T. *et al.* A potent anti-malarial human monoclonal antibody targets circumsporozoite protein minor repeats and neutralizes sporozoites in the liver. *Immunity* **53**, 733-744.e8 (2020).
15. Kisalu, N. K. *et al.* A human monoclonal antibody prevents malaria infection by targeting a new site of vulnerability on the parasite. *Nat. Med.* **24**, 408–416 (2018).
16. Zeeshan, M. *et al.* Genetic variation in the Plasmodium falciparum circumsporozoite protein in India and its relevance to RTS,S malaria vaccine. *PLoS One* **7**, e43430 (2012).
17. Weber, J. L. & Hockmeyer, W. T. Structure of the circumsporozoite protein gene in 18 strains of Plasmodium falciparum. *Mol. Biochem. Parasitol.* **15**, 305–316 (1985).
18. Oyen, D. *et al.* Structural basis for antibody recognition of the NANP repeats in *Plasmodium falciparum* circumsporozoite protein. *Proc. Natl. Acad. Sci. U.S.A.* **114**, E10438–E10445 (2017).
19. Flores-Garcia, Y. *et al.* Optimization of an in vivo model to study immunity to Plasmodium falciparum pre-erythrocytic stages. *Malar. J.* **18**, 426 (2019).
20. Kelley, B., Renshaw, T. & Kamarck, M. Process and operations strategies to enable global access to antibody therapies. *Biotechnol. Progress* **37**, e3139 (2021).
21. World Health Organization. *Preferred product characteristics: monoclonal antibodies for malaria prevention*. https://www.who.int/news-room/articles-detail/preferred-product-characteristics-monoclonal-antibodies-for-malaria-prevention.
22. Regules, J. A. *et al.* Fractional third and fourth dose of RTS,S/AS01 malaria candidate vaccine: A phase 2a controlled human malaria parasite infection and immunogenicity study. *J. Infect. Dis.* **214**, 762–771 (2016).
23. Triller, G. *et al.* Natural parasite exposure induces protective human anti-malarial antibodies. *Immunity* **47**, 1197-1209.e10 (2017).
24. Tan, J. *et al.* A public antibody lineage that potently inhibits malaria infection through dual binding to the circumsporozoite protein. *Nat. Med.* **24**, 401–407 (2018).
25. Imkeller, K. *et al.* Antihomotypic affinity maturation improves human B cell responses against a repetitive epitope. *Science* **360**, 1358–1362 (2018).
26. Murugan, R. *et al.* Evolution of protective human antibodies against Plasmodium falciparum circumsporozoite protein repeat motifs. *Nat. Med.* **26**, 1135–1145 (2020).

27. Cox, R. J. *et al.* An early humoral immune response in peripheral blood following parenteral inactivated influenza vaccination. *Vaccine* **12**, 993–999 (1994).
28. Radbruch, A. *et al.* Competence and competition: the challenge of becoming a long-lived plasma cell. *Nat. Rev. Immunol.* **6**, 741–750 (2006).
29. Nutt, S. L., Hodgkin, P. D., Tarlinton, D. M. & Corcoran, L. M. The generation of antibody-secreting plasma cells. *Nat. Rev. Immunol.* **15**, 160–171 (2015).
30. Foquet, L. *et al.* Vaccine-induced monoclonal antibodies targeting circumsporozoite protein prevent Plasmodium falciparum infection. *J. Clin. Invest.* **124**, 140–144 (2014).
31. Flores-Garcia, Y. *et al.* The P. falciparum CSP repeat region contains three distinct epitopes required for protection by antibodies in vivo. *PLoS Pathog.* **17**, e1010042 (2021).
32. Raghunandan, R. *et al.* Characterization of two in vivo challenge models to measure functional activity of monoclonal antibodies to Plasmodium falciparum circumsporozoite protein. *Malar. J.* **19**, 113 (2020).
33. Jacobi, A. M. *et al.* Correlation between circulating CD27 ^{high} plasma cells and disease activity in patients with systemic lupus erythematosus: CD27 ^{High} Plasma Cells and SLE Disease Activity. *Arthritis & Rheum.* **48**, 1332–1342 (2003).
34. Höfer, T. *et al.* Adaptation of humoral memory. *Immunol. Rev.* **211**, 295–302 (2006).
35. Chappel, J. A., Rogers, W. O., Hoffman, S. L. & Kang, A. S. Molecular dissection of the human antibody response to the structural repeat epitope of Plasmodium falciparum sporozoite from a protected donor. *Malar. J.* **3**, 28 (2004).
36. Chatterjee, D. *et al.* Avid binding by B cells to the Plasmodium circumsporozoite protein repeat suppresses responses to protective subdominant epitopes. *Cell Rep.* **35**, 108996 (2021).
37. Livingstone, M. C. *et al.* In vitro and in vivo inhibition of malaria parasite infection by monoclonal antibodies against Plasmodium falciparum circumsporozoite protein (CSP). *Sci. Rep.* **11**, 5318 (2021).
38. Dennison, S. M. *et al.* Breadth of human monoclonal antibodies isolated from RTS,S/AS01 vaccinees binding to Plasmodium falciparum circumsporozoite protein antigens. *Biophys. J.* **116**, 480a (2019).
39. Pholcharee, T. *et al.* Diverse antibody responses to conserved structural motifs in Plasmodium falciparum circumsporozoite protein. *J. Mol. Biol.* **432**, 1048–1063 (2020).
40. Wang, L. T. *et al.* Protective effects of combining monoclonal antibodies and vaccines against the Plasmodium falciparum circumsporozoite protein. *PLoS Pathog.* **17**, e1010133 (2021).
41. Pholcharee, T. *et al.* Structural and biophysical correlation of anti-NANP antibodies with in vivo protection against P. falciparum. *Nat. Commun.* **12**, 1063 (2021).
42. Langowski, M. D. *et al.* Restricted valency (NPNA)n repeats and junctional epitope-based circumsporozoite protein vaccines against Plasmodium falciparum. *NPJ Vaccines* **7**, 13 (2022).
43. Murugan, R. *et al.* Clonal selection drives protective memory B cell responses in controlled human malaria infection. *Sci. Immunol.* **3**, eaap8029 (2018).

44. McNamara, H. A. *et al.* Antibody feedback limits the expansion of B cell responses to malaria vaccination but drives diversification of the humoral response. *Cell Host & Microbe* **28**, 572-585.e7 (2020).
45. Vijayan, K. *et al.* Antibody interference by a non-neutralizing antibody abrogates humoral protection against Plasmodium yoelii liver stage. *Cell Rep.* **36**, 109489 (2021).
46. Vijay, R. *et al.* Infection-induced plasmablasts are a nutrient sink that impairs humoral immunity to malaria. *Nat. Immunol.* **21**, 790–801 (2020).
47. Oyen, D. *et al.* Cryo-EM structure of *P. falciparum* circumsporozoite protein with a vaccine-elicited antibody is stabilized by somatically mutated inter-Fab contacts. *Sci. Adv.* **4**, eaau8529 (2018).
48. Xu, Y. *et al.* Structure, heterogeneity and developability assessment of therapeutic antibodies. *mAbs* **11**, 239–264 (2019).
49. Zalevsky, J. *et al.* Enhanced antibody half-life improves in vivo activity. *Nat Biotechnol.* **28**, 157–159 (2010).
50. Kurtovic, L. *et al.* Multifunctional antibodies are induced by the RTS,S malaria vaccine and associated with protection in a phase 1/2a trial. *J. Infect. Dis.* **224**, 1128–1138 (2021).
51. White, M. T. *et al.* The Relationship between RTS,S Vaccine-Induced Antibodies, CD4+ T Cell Responses and Protection against Plasmodium falciparum Infection. *PLoS ONE* **8**, e61395 (2013).
52. Kester, K. E. *et al.* A phase I/IIa safety, immunogenicity, and efficacy bridging randomized study of a two-dose regimen of liquid and lyophilized formulations of the candidate malaria vaccine RTS,S/AS02A in malaria-naïve adults. *Vaccine* **25**, 5359–5366 (2007).
53. Ockenhouse, C. F. *et al.* Ad35.CS.01 - RTS,S/AS01 Heterologous Prime Boost Vaccine Efficacy against Sporozoite Challenge in Healthy Malaria-Naïve Adults. *PLoS ONE* **10**, e0131571 (2015).
54. Chaudhury, S. *et al.* The biological function of antibodies induced by the RTS,S/AS01 malaria vaccine candidate is determined by their fine specificity. *Malar. J.* **15**, 301 (2016).
55. Pallikkuth, S. *et al.* A delayed fractionated dose RTS,S AS01 vaccine regimen mediates protection via improved T follicular helper and B cell responses. *eLife* **9**, e51889 (2020).
56. Langowski, M. D. *et al.* Optimization of a Plasmodium falciparum circumsporozoite protein repeat vaccine using the tobacco mosaic virus platform. *Proc. Natl. Acad. Sci. U S A* **117**, 3114–3122 (2020).
57. Chatterjee, D. & Cockburn, I. A. The challenges of a circumsporozoite protein-based malaria vaccine. *Expert Rev. Vaccines* **20**, 113–125 (2021).
58. Cockburn, I. A. & Seder, R. A. Malaria prevention: from immunological concepts to effective vaccines and protective antibodies. *Nat. Immunol.* **19**, 1199–1211 (2018).
59. Wang, L. T. *et al.* The light chain of the L9 antibody is critical for binding circumsporozoite protein minor repeats and preventing malaria. *Cell Rep.* **38**, 110367 (2022).
60. Calvo-Calle, J. M., Mitchell, R., Altszuler, R., Othoro, C. & Nardin, E. Identification of a neutralizing epitope within minor repeat region of Plasmodium falciparum CS protein. *NPJ Vaccines* **6**, 10 (2021).

61. Schofield, L. The circumsporozoite protein of Plasmodium: a mechanism of immune evasion by the malaria parasite? *Bull. World Health Organ.* **68**, 66–73 (1990).

62. Schofield, L. On the function of repetitive domains in protein antigens of Plasmodium and other eukaryotic parasites. *Parasitology Today* **7**, 99–105 (1991).

Figures

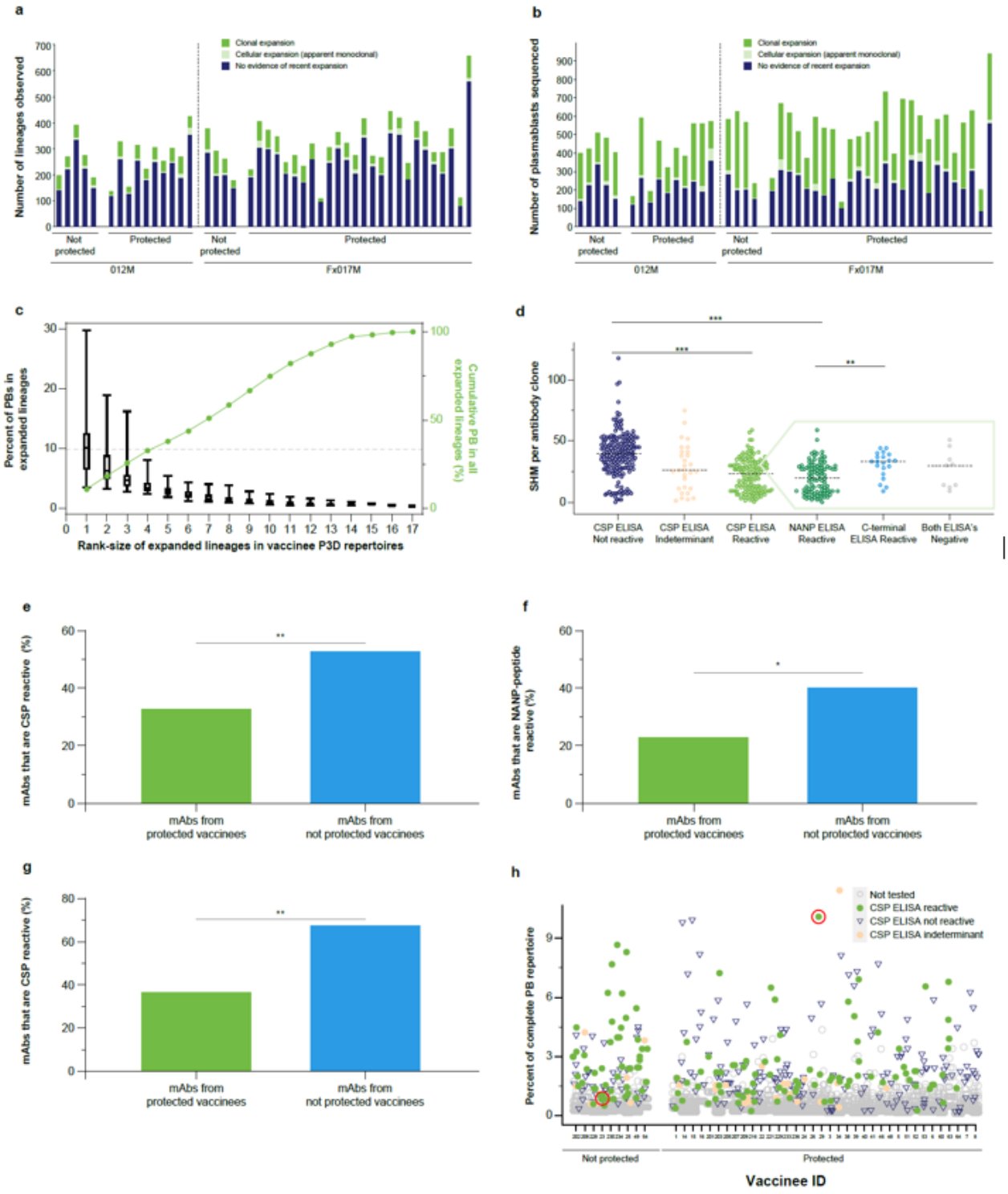

Figure 1

CSP-reactive lineages from blood PBs after the third dose of RTS,S. a–b, IgG lineages for each vaccinee (bars, *n* = 45) that are clonally expanded (green), that are cellularly expanded but with only one IgG clone observed (grey), or that lack evidence of recent expansion and contain only one observed PB (blue) are shown by, a, number of lineages or, b, number of PBs per vaccinee. c, By vaccinee, the size of each expanded lineage was calculated by dividing the number of PBs in that lineage by the number of PBs in all expanded lineages within each repertoire and then assigning a rank-size. Boxes indicate interquartile ranges, lines within boxes are medians, and whiskers represent minimum and maximum across vaccinees for each rank-size, with the top four rank-size lineages containing 33% of PBs in all expanded lineages (dotted line). d–g, ELISA reactivity, SHM levels and vaccinee protection status of mAbs from expanded lineages (*n* = 349). d, Distribution of SHM levels for mAbs that are not reactive (dark blue, *n* = 185), show indeterminant, weak signal (orange, *n* = 29), or are reactive (light green, *n* = 135) in a CSP ELISA. Domain specificity for CSP-reactive mAbs is shown in the light green box. Monoclonal antibodies reactive by ELISA to NANP6 repeat-region peptide (light green, *n* = 98), to the C-terminal region peptide (Pfs16, light blue, *n* = 20), or that are not reactive in either peptide ELISA (light green, *n* = 9), lines are medians, ***$P < 0.0001$, **$P < 0.001$, unpaired two-tailed Mann–Whitney test. CSP-reactive mAbs that were not tested in peptide ELISAs (*n* = 8) are not shown. e–g, Percent of tested antibodies from expanded lineages that originate from protected (green, *n* = 36) and not protected (blue, *n* = 9) vaccinees that are, e, CSP-reactive (82/249 and 53/100 mAbs, respectively), f, repeat-region, NANP6 peptide-reactive (59/244 and 39/97 mAbs, respectively), and, g, the subset from just the dominant rank-size 1–4 lineages that are CSP-reactive (52/142 and 31/46 mAbs, respectively), **$P < 0.001$, *$P < 0.01$, Fisher's exact test. h, For vaccinees shown on the x-axis, each symbol indicates a single lineage. The lineages (*n* = 369) from which a clone was selected for testing are indicated by CSP reactivity: CSP-reactive (green dots, *n* = 139), indeterminant (orange dots, *n* = 29), or not reactive (blue triangles, *n* = 201). All lineages that were not tested are shown (grey circles, *n* = 13,134; 2,313 expanded and 10,821 single-PB lineages). Protected vaccinees have a lower ratio of CSP-reactive versus non-reactive lineages than not protected vaccinees (bootstrap analysis, $P = 0.0011$). Red circles indicate the two lineages that contain the peptide mAb clone of AB-000317.

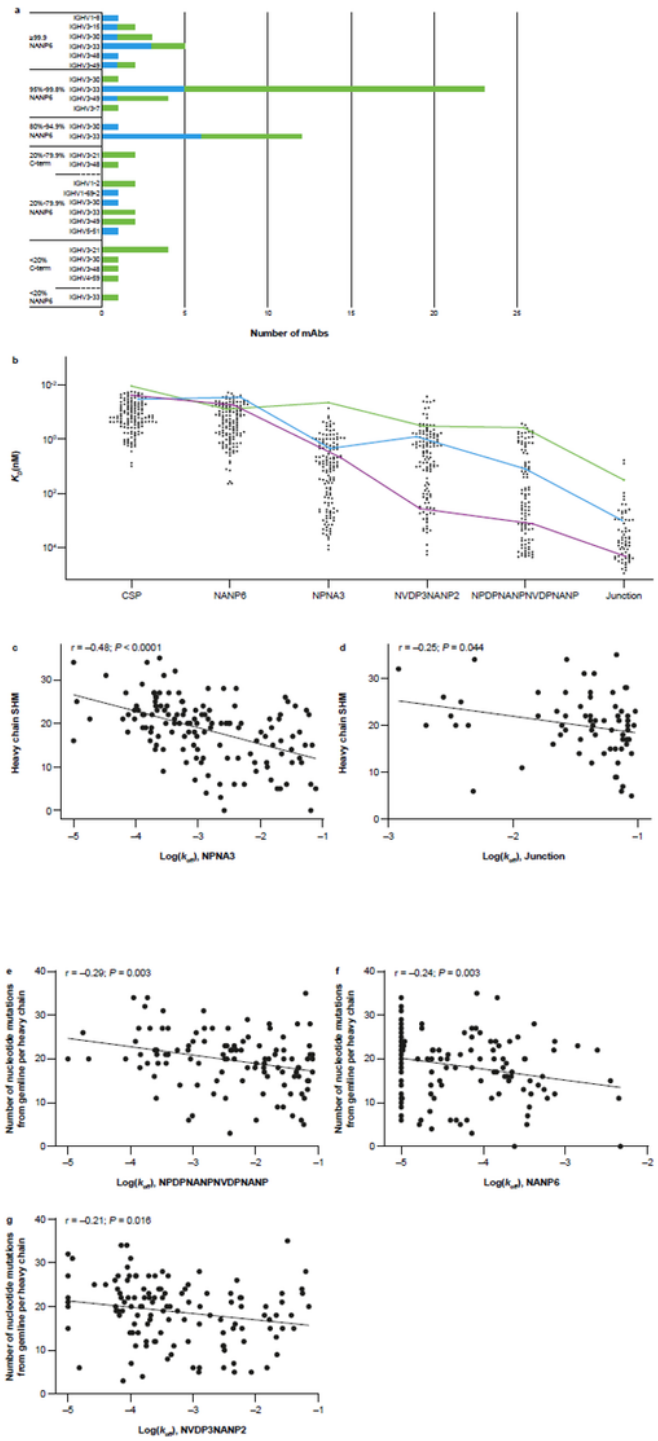

Figure 2

Functional mAbs bind CSP-derived peptides not present in RTS,S. a, Monoclonal antibodies were grouped together by percent inhibition in the sporozoite liver burden murine challenge model, and sub-categorized first by binding specificity and further sub-categorised by mAb IGHV. Antibodies derived from protected vaccinees are green (n = 54), and from not protected vaccinees are blue (n = 23). b, SPR-determined binding potencies (K_D) of mAbs (n = 141) selected from 35 of the most efficacious lineages tested

against CSP and a panel of CSP-derived peptides that are homologous (NANP6, NPNA3) or heterologous (NVDP3NANP2, NPDPNANPNVDPNANP, Junction) to RTS,S. Examples are shown of a mAb with a broadly promiscuous binding profile (green, AB-007163), a mAb with a profile relatively biased to homologous peptides (purple, AB-007143), and one with a profile in between these extremes (blue, AB-007175). c–g, Linear regression of log-transformed data comparing heavy chain SHM of mAbs versus SPR binding off-rate (k_{off}) against peptides, c, NPNA3 (n = 140), d, junction (KQPADGNPDPNANPN, n = 68), e, NPDPNANPNVDPNANP (n = 109), f, NANP6 (n = 141), and, g, NVDP3NANP2 (n = 129). For correlations of non-transformed data, P < 0.03 for all comparisons (Spearman test), and P < 0.04 for all comparisons (Pearson test) except P = 0.6 for NVDP3NANP2, see Extended Data Table 1.

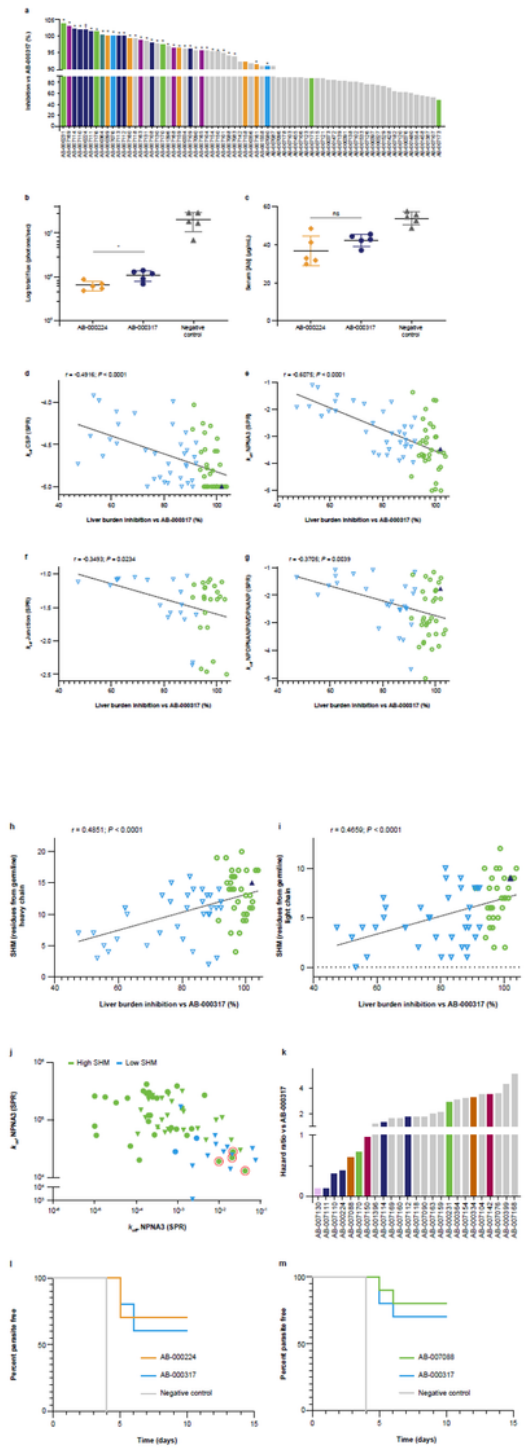

Figure 3

In vivo pharmacology, SHM, and binding of mAbs prioritised for development. a–c, Liver burden model, a, percent inhibition compared to untreated, infected mice (geometric mean, n = 5, 100µg/mouse) and normalised to the activity of AB-000317 of n = 69 antibodies (32 lineages) with colours other than grey indicating the six lineages that contain the most efficacious mAbs (*P > 0.05, †P < 0.05, two-sided, non-parametric log-rank), and, b–c, example data from AB-000224 and AB-000317 of, b, parasite

bioluminescence in the liver (total flux, photons/sec), *P = 0.03, and, c, serum concentrations (Serum[Ab], μg/ml) of mAb at time of sporozoite challenge, P > 0.2 ("ns"), mean±SD (n = 5 mice), two-tailed Mann–Whitney test. d–i, Percent liver burden inhibitory activity compared to untreated, infected mice (geometric mean, n = 5) and normalised to the activity of AB-000317 with each mAb indicated as having activity significantly better (dark blue triangle), not different (green circles), or weaker (light blue triangles) than AB-000317 (two-sided, non-parametric log-rank) versus d–g, binding off-rate (SPR, k_{off}) against, d, CSP (n = 70), e, major repeat (NPNA3, n = 70), f, junctional (KQPADGNPDPNANPN, n = 42), and, g, minor repeat (NPDPNANPNVDPNANP, n = 60) peptides, and versus, h–i, the number of amino acid residue changes from SHM for each mAb's (n = 70), h, heavy and, i, light chain, linear regression of log-transformed data is shown. For correlations of non-transformed data, P < 0.005 for all comparisons (Pearson test), and P < 0.05 for all comparisons (Spearman test) except P = 0.06 for liver burden inhibition versus, g, k_{off} [NPDPNANPNVDPNANP], see Extended Data Table 1. j, SPR binding off- (k_{off}) versus on-rates (k_{on}) against NPNA3 peptide of mAbs with high SHM (green, ≥20 mutations per clone, n = 56) or low SHM (blue, <20 mutations per clone, n = 14) and with activity weaker (down triangles), no different (circles), or better (up triangle) than AB-000317 (two-sided, non-parametric log-rank). Monoclonal antibodies from a lineage reported to bind CSP with Fab–Fab homotypic interactions indicated (red circles, AB-000399[41] AB-007159, AB-007160, AB-007161). k, Hazard ratios of n = 25 antibodies (14 lineages) compared to AB-000317 in the mosquito-bite parasitaemia model (n = 10 mice, 150μg/mouse) with colours other than grey indicating the five lineages that contain the most efficacious antibodies, and, l-m, survival curves from repeat experiments in comparison to AB-000317 of, l, AB-000224 [0.74 (0.15, 3.8)] and, m, AB-007088 [0.61 (0.097, 3.8)], n = 10 mice, two-sided, non-parametric log-rank [Mantel–Haenszel hazard ratio (95% confidence intervals)].

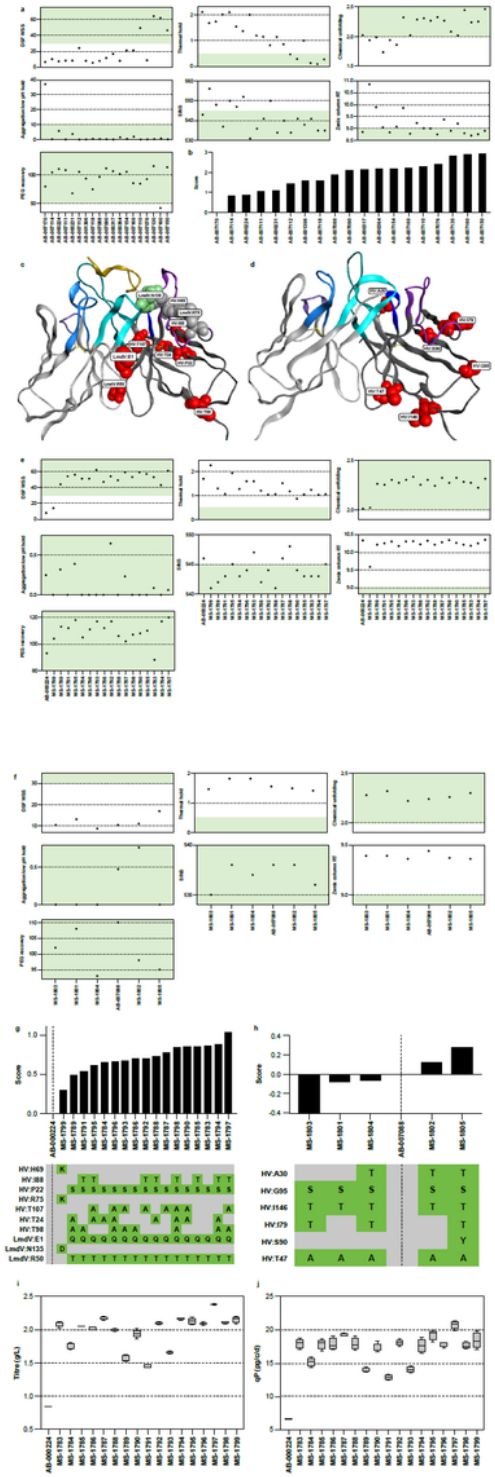

Figure 4

Developability properties of lead antibodies and engineered variants for development. a–b, Developability properties of prioritised, lead antibodies as characterised by, a, scores from differential scanning fluorimetry (DSF WSS), thermal hold, chemically induced unfolding, low pH stability (aggregate low pH hold) self-interaction nanoparticle spectroscopy (SINS), stand-up monolayer affinity chromatography (Zenix column RT), relative solubility analysis (PEG recovery), and, b, relative, aggregate scores from

assay panel results. c–d, Mutations made to generate engineered variants depicted on the Fv region of, c, the Fab of AB-000224 in complex with NPNA4 (gold ribbon, PDB ID 6WFY, *see Methods*), and of, d, a Fab structure model of AB-0007088 built in the MOE Antibody Modeler (*see Methods*). The light chain framework is in silver and the heavy chain in dim grey. The CDRs for light and heavy chains are indicated, respectively, as CDR1 (light and dark blue), CDR2 (light and dark purple), and CR3 (light and dark cyan). Mutation sites of engineered variants are labelled as stability violations (red), deamidation site (green) and paired sibling sites (grey, *see Methods*). e–h, Developability properties of engineered variants for, e, g, the lead candidate, AB-000224, and, f, h, backup, AB-007088, in, e–f, the assays listed for panel a,and, g–h, the aggregate scores from assay panel results in comparison to the respective parental antibody with mutations of the variant compared to the parental indicated. i–j, Characterisation of stable cell production pools generated from engineered variants compared to parental AB-000224 for, i, production titres, (Titre, g/L) and, j, cell-specific productivity (qP, pg per cell per day). Boxes indicate interquartile ranges, lines within boxes are medians, and whiskers represent minimum and maximum across replicate pools (3-5 per engineered variant).

Supplementary Files

This is a list of supplementary files associated with this preprint. Click to download.

- SupplementaryTable1Anantibodydrugformalaria.xlsx
- SupplementaryTable2Anantibodydrugformalaria.xlsx
- SupplementaryTable3Anantibodydrugformalaria.xlsx
- SupplementaryTable4Anantibodydrugformalaria.xlsx
- SupplementaryTable5Anantibodydrugformalaria.xlsx
- SupplementaryTable6Anantibodydrugformalaria.xlsx
- SupplementaryTable7Anantibodydrugformalaria.xlsx
- Extendeddata.docx